SAND--89-0326C

DE89 010436

TWO MAPPING TECHNIQUES FOR CALCULATING RADIATIVE HEAT TRANSFER WITH SCATTERING*

by

W. C. A. Gu** and K. K. Murata

Sandia National Laboratories
Albuquerque, New Mexico 87185

DISCLAIMER

---

*This work is supported by the United States Nuclear Regulatory Commission under FIN A1198 and was performed at Sandia National Laboratories, which is operated for the United States Department of Energy under contract number DE-AC04-76DP00789

**Jack Tills and Associates, Inc., Albuquerque, New Mexico 87110

ABSTRACT

The problem of radiative heat transfer through a gray, emitting, absorbing, and scattering medium with uniform optical properties is reduced to one without scattering through two techniques. One uses scaling laws, and the other uses a self-consistent effective gas temperature. The scaling laws are derived via the P_1 approximation to the radiative transfer equation and can be applied to multidimensional problems with nonisothermal media. The effective temperature method is presently restricted to isotropic scattering and isothermal media. Both methods are evaluated in the current study as a function of scattering albedo, wall emissivity, and optical thickness for two different geometries, and two sets of wall and gas temperatures. The effects of scattering anisotropy are also assessed for the P_1 method. The numerical results show that for these cases the scaling method is reasonably accurate for optically thick media with a scattering albedo less than 0.8, and the effective temperature technique is reasonably accurate for optically thin media for all albedos.

NOMENCLATURE

D = diffusion coefficient, m
I = radiation angular intensity, W/m^2-sr
$\hat{n}_w$ = outward unit vector normal to a surface element
P = scattering phase function
q = radiant heat flux, W/m^2
r = radial coordinate, m
s = surface area, m^2
S = total surface area, m^2
T = temperature, K
v = volume, m^3
V = total volume, m^3

Greek Symbols

ϵ = emissivity
θ_o = scattering angle
μ = angular coordinate, see Fig. 1
$\bar{\mu}_o$ = average cosine of the scattering angle
ξ = optical depth
ρ = reflectivity
σ = attenuation coefficient due to radiation/media interactions, m^{-1}

$\hat{\sigma}$ = Stefan-Boltzmann constant, W/m^2-K^4
ϕ = scalar flux of thermal radiation, W/m^2
$\tilde{\phi}$ = volume-averaged scalar flux, W/m^2
ω = scattering albedo
$\hat{\Omega}$ = solid angle

Subscripts

a = absorption
e = extinction
eff = net efflux of thermal radiation
m = medium property
s = scattering
t = total length
w = wall property
1 = boundary index
2 = boundary index

Superscripts

' = angular coordinate of the scattering direction, or the effective temperature

1. INTRODUCTION

Radiative heat transfer is one of the dominant modes of heat transfer in many engineering applications involving high temperatures. For radiative transfer through purely gaseous media, the effects of scattering are negligible in most heat transfer calculations due to the fact that the interactions between the thermal radiation and gas molecules or atoms occur in the Rayleigh limit. In this limit scattering is negligible compared to the absorption and transmission of radiation. However, in the presence of suspended solid or liquid aerosol particles, scattering often must be considered.

By nature, the equation of radiative transfer with scattering is an integro-differential equation whose solution is quite difficult. Although advanced numerical solution techniques are available for solving the general equation such as the P_n method (e.g., Bell and Glasstone, 1970), the discrete ordinates or the S_n method (e.g., Bell and Glasstone, 1970), and the Monte Carlo method (Meyer, 1956), such detailed numerical solutions are not warranted in many practical applications for a number of reasons. First, the solution of the radiative transfer equation is quite sensitive to the optical properties of the transport medium and

such optical properties for materials of interest are seldom available in the literature, (e.g., the complex indices of refraction for most dielectric materials are only reported for visible light at room temperature.) Even if the indices of refraction are known, the shape, chemical structure, and size distribution of the aerosols may not be known accurately. Assuming this information were available, in some applications one cannot afford computationally to take the resulting wavelength dependence of the optical properties into account with high accuracy. Second, the results of radiant energy exchange are of little use in many cases without considering simultaneously the thermal-hydraulic response of the system to the radiation. The solution of the coupled problem can be a formidable task.

The above considerations indicate that methods for solving the scattering problem to moderate accuracy may be quite useful if they are efficient. The present paper proposes and gives the results of a preliminary study for two such methods. These methods have been developed for potential use with CONTAIN, a code that can analyze coupled aerosol, fission product, and thermal-hydraulic behavior in severe nuclear reactor accidents (Murata et al., 1989). The radiative transport problem is solved every timestep in this code, and consequently there is a premium on computational efficiency.

Methods with moderate accuracy similar to one of the present methods have been proposed before. The equation of radiative transfer reduces to a differential equation when scattering is absent so that the effort required to solve the problem is reduced considerably. Although scattering itself often cannot be neglected in the presence of aerosols, one can take an unconventional approach to the transport problem with scattering by first mapping it onto a nonscattering one, and then seeking the solution of the mapped problem. Such approaches have been reported in the literature (Goswami and Vachon, 1977; Lee and Buckius, 1982, 1983, and 1986). The basis of these earlier approaches is either the P_1 approximation to the transport equation or the two-flux method.

In the present study, two complementary mapping methods have been developed for potential application to the multidimensional problem, one using the P_1 approximation and the other using an effective medium temperature. The P_1 mapping is derived by requiring the P_1 solutions of the original and the mapped problems to be identical and can be applied to multidimensional problems with nonisothermal media. While similar to the P_1 approach used in Lee and Buckius (1983), the present approach has a number of advantages. First, when the equation for the scalar flux is scaled, as in the present approach, rather than that for the heat flux, it becomes apparent that nonisothermal media can be treated. (The difficulty is that the temperature gradient term in the heat flux equation introduces a second dimensionless group.) Second, when gray wall boundary conditions are used, a factor containing the wall emissivity can be combined with a second dimensionless group introduced by the boundary conditions. Because there are two parameters to scale in the present treatment (the optical depth and the wall emissivity), the scaling difficulties found by Lee and Buckius to arise from the presence of two dimensionless groups are absent, and the present method is exact within the P_1 approximation.

It is well known that the P_1 approximation is poor when the optical thickness of the system decreases (Duderstadt and Hamilton, 1976). Unfortunately, the proposed P_1 scaling laws transform the original problem with a high scattering albedo into an optically thin problem. Therefore, it is expected that the current P_1 mapping method will fail in two circumstances: (1) for optically thin systems, and (2) for high scattering albedos. (It should be noted that in contrast the P_1 approximation itself generally improves with scattering albedo at fixed optical depth.)

A second mapping method, an effective temperature method, has been developed for optically thin systems. In the effective temperature method, the emission and the scattering terms of the radiative transfer equation are combined into an effective emission term characterized by an effective emission temperature. Generally, this effective emission temperature is unknown and must be obtained by iteration.

Both the P_1 mapping technique and the effective temperature method have been assessed through a number of calculations for isothermal media comparing the mapped solutions with those obtained by a reference discrete ordinates method. While the generality of these results remains to be demonstrated, the results for the cases investigated indicate that the P_1 mapping method will result in less than 5 percent error in the net efflux of radiation (defined in Eq. (19)) for an optical depth greater than 4 and a scattering albedo less than 0.8, while the effective temperature method will result in less than 5 percent error for an optical depth less than 4. Furthermore, the error in both mapping methods is improved considerably when the transport medium is surrounded by reflective (nonblack) boundaries.

2. THEORY

The P_1 approximation to the radiative transfer equation can be derived by taking the zeroth and the first moments of the radiative transfer equation and assuming that the angular intensity is at most linearly anisotropic (see, for example, Duderstadt and Hamilton, 1976). The present scaling method uses the P_1 scalar flux equation, i.e.,

$$-D\nabla^2\phi(\vec{r})+\sigma_a\phi(\vec{r})=4\sigma_a\hat{\sigma}T^4(\vec{r}) \quad . \tag{1}$$

It should be noted that Eq. (1) applies only to a gray medium with uniform optical properties. The boundary condition for a diffusely reflecting wall in the P_1 approximation can be written as

$$D\vec{\nabla}\phi(\vec{r}_w)\cdot\hat{n}_w=\frac{\epsilon_w}{2(1+\rho_w)}\phi(\vec{r}_w)-\frac{2\epsilon_w}{1+\rho_w}\hat{\sigma}T_w^4 \quad , \tag{2}$$

where D is the diffusion coefficient defined as

$$D=[3(\sigma_s-\bar{\mu}_o\sigma_s)]^{-1} \quad , \tag{3}$$

and $\bar{\mu}_o$ is the first moment of the scattering phase function.

In the first mapping method, the original problem with scattering is solved by assuming that it is equivalent to a nonscattering one. The P_1 equation and the boundary condition for the mapped problem without scattering can be written as

$$-\bar{D}\nabla^2\bar{\phi}(\vec{r})+\bar{\sigma}_a\bar{\phi}(\vec{r})=4\bar{\sigma}_a\hat{\sigma}T^4(\vec{r}) \quad , \tag{4}$$

and

$$\bar{D}\vec{\nabla}\bar{\phi}(\vec{r}_w)\cdot\hat{n}_w=\frac{\bar{\epsilon}_w}{2(1+\bar{\rho}_w)}\bar{\phi}(\vec{r}_w)-\frac{2\bar{\epsilon}_w}{1+\bar{\rho}_w}\hat{\sigma}T_w^4 \quad , \tag{5}$$

where

$$\bar{D}=(3\bar{\sigma}_a)^{-1} \quad , \tag{6}$$

and the bar indicates the mapped quantities. The solutions for ϕ in the original and mapped problems are identical, if and only if, the following relations are satisfied:

$$\frac{\sigma_a}{D}=\frac{\bar{\sigma}_a}{\bar{D}} \quad , \tag{7}$$

and

$$\frac{\epsilon_w}{D(1+\rho_w)}=\frac{\bar{\epsilon}_w}{\bar{D}(1+\bar{\rho}_w)} \quad . \tag{8}$$

Therefore after rearrangement, the scaling laws given by Eqs. (7) and (8) can be written as:

$$\bar{\sigma}_a=\sigma_e\sqrt{(1-\omega)(1-\bar{\mu}_o\omega)} \quad , \tag{9}$$

and

$$\bar{\rho}_w=2\left[1+\sqrt{\frac{1-\bar{\mu}_o\omega}{1-\omega}}\,\frac{\epsilon_w}{1+\rho_w}\right]^{-1}-1 \quad , \tag{10}$$

where ω is the single scattering albedo σ_s/σ_a. It should be noted that $\bar{\rho}_w$ may be negative, in which case the corresponding wall emissivity is greater than one. (The solutions for ϕ in this case are not unphysical because they correspond to the original problem with a

properly bounded emissivity.) Eq. (9) is equivalent to the square-root scaling law derived by Lee and Buckius (1982, 1983).

Finally, since $\vec{q}(\vec{r})$ and $\phi(\vec{r})$ are related in the P_1 approximation according to

$$\vec{q}(\vec{r}) = -D\vec{\nabla}\phi(\vec{r}) \quad , \tag{11}$$

the radiant energy flux of the original problem is given by

$$[\vec{q}(\vec{r})]_{\text{original}} = \sqrt{\frac{1-\omega}{1-\bar{\mu}_0\omega}}\,[\vec{q}(\vec{r})]_{\text{mapped}} \quad . \tag{12}$$

The second mapping method, or the effective temperature method, applies to problems with isotropic scattering. It is assumed here for simplicity that the medium temperature and effective temperature are constant. (This assumption can be relaxed through a generalization of the equations below.) For an isotropic scattering medium, the scattering integral in the radiative transfer equation, Eq. (A-1), reduces to $\sigma_s\phi(\vec{r})/4\pi$, and the right-hand side of Eq. (A-1) becomes independent of angle. Furthermore, if the optical depth is small and the spatial variation of the scattered flux is small, it is possible to represent the total radiation source (emission and scattering) with an effective radiation source characterized by an effective emission temperature T':

$$\frac{\sigma_a}{\pi}\hat{\sigma}T^4 + \frac{\sigma_s}{4\pi}\phi(\vec{r}) = \frac{\sigma_e}{\pi}\hat{\sigma}(T')^4 \quad . \tag{13}$$

The radiative transfer equation for the mapped problem thus becomes a nonscattering one:

$$\hat{\Omega}\cdot\vec{\nabla}I(\vec{r},\hat{\Omega}) + \sigma_e I(\vec{r},\hat{\Omega}) = \frac{\sigma_e}{\pi}\hat{\sigma}(T')^4 \quad . \tag{14}$$

Generally, the effective temperature is unknown and must be found by iteration. It is defined implicitly by the volume averages of the radiation flux equation and Eq. 13. The radiation flux equation is obtained by integrating Eq. (14) over all solid angles, which results in

$$\vec{\nabla}\cdot\vec{q}(\vec{r})+\sigma_e\phi(\vec{r})=4\sigma_e\hat{\sigma}(T')^4 \quad . \tag{15}$$

From the divergence theorem, the volume-averaged scalar flux is found to be

$$\bar{\phi}=4\hat{\sigma}(T')^4-\frac{1}{\sigma_e V}\oint_S \vec{q}(\vec{r})\cdot d\vec{s} \quad . \tag{16}$$

The volume average of Eq. (13) gives

$$(T')^4=(1-\omega)T^4+\frac{\omega}{4\hat{\sigma}}\bar{\phi} \quad . \tag{17}$$

Therefore, one may write

$$T^4-(T')^4=\frac{\omega}{4\hat{\sigma}\sigma_e V(1-\omega)}\oint_S \vec{q}(\vec{r})\cdot d\vec{s} \quad . \tag{18}$$

Equation (18) defines T' implicitly and is solved iteratively for T'.

In the next section, the two mapping methods will be assessed against more exact numerical methods.

3. EVALUATION

To examine the validity of both the P_1 mapping technique and the effective temperature method, one-dimensional planar and spherical geometries are studied quantitatively. Figure 1 summarizes the coordinate systems used in the following calculations.

In the following assessment of the mapping methods, the original problems with scattering and the mapped problems without scattering were all solved by an S_{32} discrete ordinates method except for the mapped problems in planar geometry. For the latter cases the well-known analytic solution was used. The discrete ordinates solutions were obtained using 32 angular directions, 201 spatial nodes, and a convergence criterion of 10^{-6} for the fractional error in angular intensities. (The P_1-mapped problem is not solved here in the P_1 approximation because in the intended application, it will not be solved in the P_1 approximation but by essentially exact net enclosure methods.)

Finally, it is assumed in the assessment that one is interested in the net radiant heat fluxes at walls, or equivalently, the volume-averaged scalar flux, $\bar{\phi}$, which is proportional to the total absorption of radiant energy by the medium. The net radiant heat fluxes at the boundaries, or efflux ϕ_{eff}, and the volume-averaged scalar flux are related by the radiation flux equation according to

$$\phi_{eff} = \frac{1}{\sigma_a V}\oint_S \vec{q}(\vec{r})\cdot d\vec{s} = 4\hat{\sigma}T_m^4 - \bar{\phi} \quad . \tag{19}$$

In view of the large number of input parameters, the physical dimensions were fixed in the calculations. They are: x_t = 1 m, r_1 = 1 m, and r_2 = 2 m. Two sets of boundary temperatures were studied: (1) $T_{w1} = T_{w2} = T_w$, and T_w/T_m = 1.5; and (2) T_{w2}/T_{w1} = 1.5, and T_{w2}/T_m = 1.2. The combinations of geometries and temperatures considered are given by the three cases listed in Table 1. Each case was evaluated for the two mapping methods as a function of wall emissivity, albedo, and optical depth. The P_1 mapping method was also evaluated for two different scattering phase functions. The first,

$$P_1(\theta_o) = 1 \quad , \tag{20}$$

represents isotropic scattering and the second,

$$P_2(\theta_o) = \frac{8}{3\pi}(\sin\theta_o - \theta_o\cos\theta_o) \quad , \tag{21}$$

represents diffuse scattering from a large sphere (Siegel and Howell, 1972). Hereafter, these two phase functions will be referred to as the isotropic scattering and anisotropic scattering phase functions, respectively.

The percentage error in the net radiation efflux is presented in Figures 2 through 8 for various wall emissivities. The percentage error of the mapping methods is defined by

$$\left|\frac{(\phi_{eff})_{mapping} - (\phi_{eff})_{Sn}}{(\phi_{eff})_{Sn}}\right| \times 100 \quad . \tag{22}$$

The coordinate ξ_t in these figures is equal to $\sigma_e x_t$ and $\sigma_e(r_2-r_1)$ in planar and spherical geometry, respectively. Error contour plots are shown for the P_1 mapping technique in Figures 2 through 5, and for the effective temperature method in Figures 6 through 8.

There are several conclusions that can be drawn from the numerical results:

1. As shown in Figures 2 through 5, the error in the efflux in the P_1 mapping method increases as the scattering albedo increases. This can be attributed to the fact that the mapped system as shown in Eq. (9) becomes optically thinner as scattering albedo increases, and the P_1 approximation is poor for an optically thin system. The errors are not a strong function of the cases and the two scattering phase functions studied. However, it remains to be seen whether the P_1 mapping method is suitable for a more irregularly shaped phase function, as found in general from Mie theory (van de Hulst, 1981). As shown in Figures 2 through 5, an error in the efflux of less than 5 percent can be expected using the P_1 mapping technique for an optical depth greater than about four, and a scattering albedo less than about 0.8.

2. As shown in Figures 6 through 8, the efflux in the effective temperature method is accurate for small to moderate values of optical thickness. For an optical thickness less than about four, the effective temperature method is very accurate for the entire range of the scattering albedos. Note that this conclusion is drawn for the efflux for the cases considered; other quantities and cases are presently under investigation.

3. The accuracy of both mapping methods studies improves considerably as the wall emissivity decreases. For a gray wall, part of the thermal radiation that reaches the boundary is reflected back into the system. As a result, radiant energy becomes more evenly distributed than it would with black walls, and consequently both methods become more suitable.

4. In Figures 2 through 5 for the P_1 mapping technique, the errors are observed to decrease sharply as the optical depth becomes extremely small. This behavior is surprizing since it is known that the P_1 approximation fails for a transparent medium. However, it can be shown that the P_1 approximation predicts the correct transparent medium wall fluxes in the limit as ξ_t approaches zero. Therefore, both the P_1 approximation and the P_1 mapping technique predict the correct behavior in this limit.

4. CONCLUSIONS

Two mapping methods based on the P_1 approximation and an effective temperature have been developed for radiative heat transfer problems with scattering. In the P_1 mapping technique, a radiative transfer problem with scattering medium is transformed into a non-scattering one by scaling the absorption coefficient and the wall emissivities within the P_1 approximation. The scaling laws thus obtained are not restricted to the one-dimensional planar geometries used in previous scaling approaches and may in principle be applied to nonisothermal problems as well. The effective temperature method applies to optically thin systems with isotropic scattering and isothermal media, provided the spatial variation of the scattered flux is small.

Both mapping methods have been examined in a number of cases involving an isothermal gas and both planar and curved geometries. Note, however, that although a large number of calculations were required to generate the results in Figures 2-8, the cases presented in this paper are not comprehensive. For example, it would be desirable to run cases with a hot gas radiating to cold walls and with a relatively small hot surface radiating to cold walls that have a much larger area. In the latter case, it is not clear that the net efflux is the appropriate quantity to use in evaluating the accuracy of the mapping methods. The errors in the transmitted flux and gas temperature under equilibrium conditions are also of interest. These other cases and quantities are presently under investigation.

It is concluded that for the cases considered the current P_1 mapping technique gives a reasonably accurate net efflux for an optical depth greater than about four and a scattering albedo less than about 0.8, and the effective temperature method gives a reasonably accurate one for an optical depth less than about four.

REFERENCES

Bell, G. I., and Glasstone, S., 1970, Nuclear Reactor Theory, Van Nostrand, Princeton, NJ.

Duderstadt, J. J., and Hamilton, L. J., 1976, Nuclear Reactor Analysis, John Wiley & Sons, Inc., New York.

Goswami, D. Y., and Vachon, R. I., 1977, "Radiative Heat Transfer Analysis Using an Effective Absorptivity for Absorption, Emission and Scattering," International Journal of Heat and Mass Transfer, Vol. 20, pp. 1233-1239.

Lee, H., and Buckius, R. O., 1982, "Scaling Anisotropic Scattering in Radiation Heat Transfer for a Planar Medium," Journal of Heat Transfer, Vol. 104, pp. 68-75.

Lee, H., and Buckius, R. O., 1983, "Reducing Scattering to Nonscattering Problems in Radiation Heat Transfer," International Journal of Heat and Mass Transfer, Vol. 26, No. 7, pp. 1055-1062.

Lee, H., and Buckius, R. O., 1986, "Combined Mode Heat Transfer Analysis Utilizing Radiation Scaling," Journal of Heat Transfer, Vol. 108, pp. 626-632.

Meyer, H. A. (ed.), 1956, Symposium on Monte Carlo Methods, John Wiley & Sons, Inc., New York.

Murata, K. K., et al., 1989, "User's Manual for CONTAIN 1.1, A Computer Code for Severe Nuclear Reactor Accident Containment Analysis," (Draft), SAND87-2309, Sandia National Laboratories, Albuquerque, NM.

Siegel, R., and Howell, J. R., 1972, Thermal Radiation Heat Transfer, McGraw-Hill Book Co., New York.

van de Hulst, H. C., 1981, Light Scattering by Small Particles, Dover Publications, Inc., New York.

APPENDIX A. THE P_1 APPROXIMATION

For a gray medium with uniform optical properties, the radiative transfer equation is given by

$$\hat{\Omega}\cdot\vec{\nabla}I(\vec{r},\hat{\Omega}) + \sigma_e I(\vec{r},\hat{\Omega}) = \frac{\sigma_s}{\pi}\hat{\sigma}T^4(\vec{r}) + \frac{\sigma_s}{4\pi}\int_{4\pi} P(\hat{\Omega}\cdot\hat{\Omega}')I(\vec{r},\hat{\Omega}')d\hat{\Omega}' \quad . \qquad (A-1)$$

For a diffuse gray isothermal surface, the boundary condition for Eq. (A-1) can be stated as follows:

$$I(\vec{r}_w,\hat{\Omega}\cdot\hat{n}_w>0) = \frac{\epsilon_w}{\pi}\hat{\sigma}T_w^4 - \frac{\rho_w}{\pi}\int_{\hat{n}_w\cdot\hat{\Omega}'<0} I(\vec{r}_w,\hat{\Omega}')\hat{n}_w\cdot\hat{\Omega}'d\hat{\Omega}' \quad , \qquad (A-2)$$

where $\hat{n}_w$ is the outward normal unit vector perpendicular to the surface element at position $\vec{r}_w$.

Table 1. Cases considered.

	Geometry	T_m	T_{w1}	T_{w2}
Case I	Planar	T_m	$1.5T_m$	$1.5T_m$
Case II	Planar	T_m	$0.8T_m$	$1.2T_m$
Case III	Spherical	T_m	$1.5T_m$	$1.5T_m$

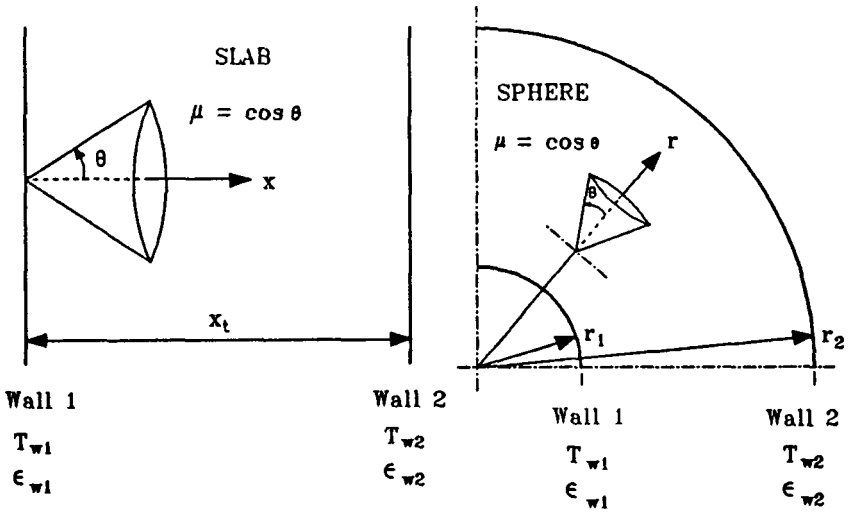

Fig. 1. Graphic representation of the coordinate systems used in the numerical calculations.

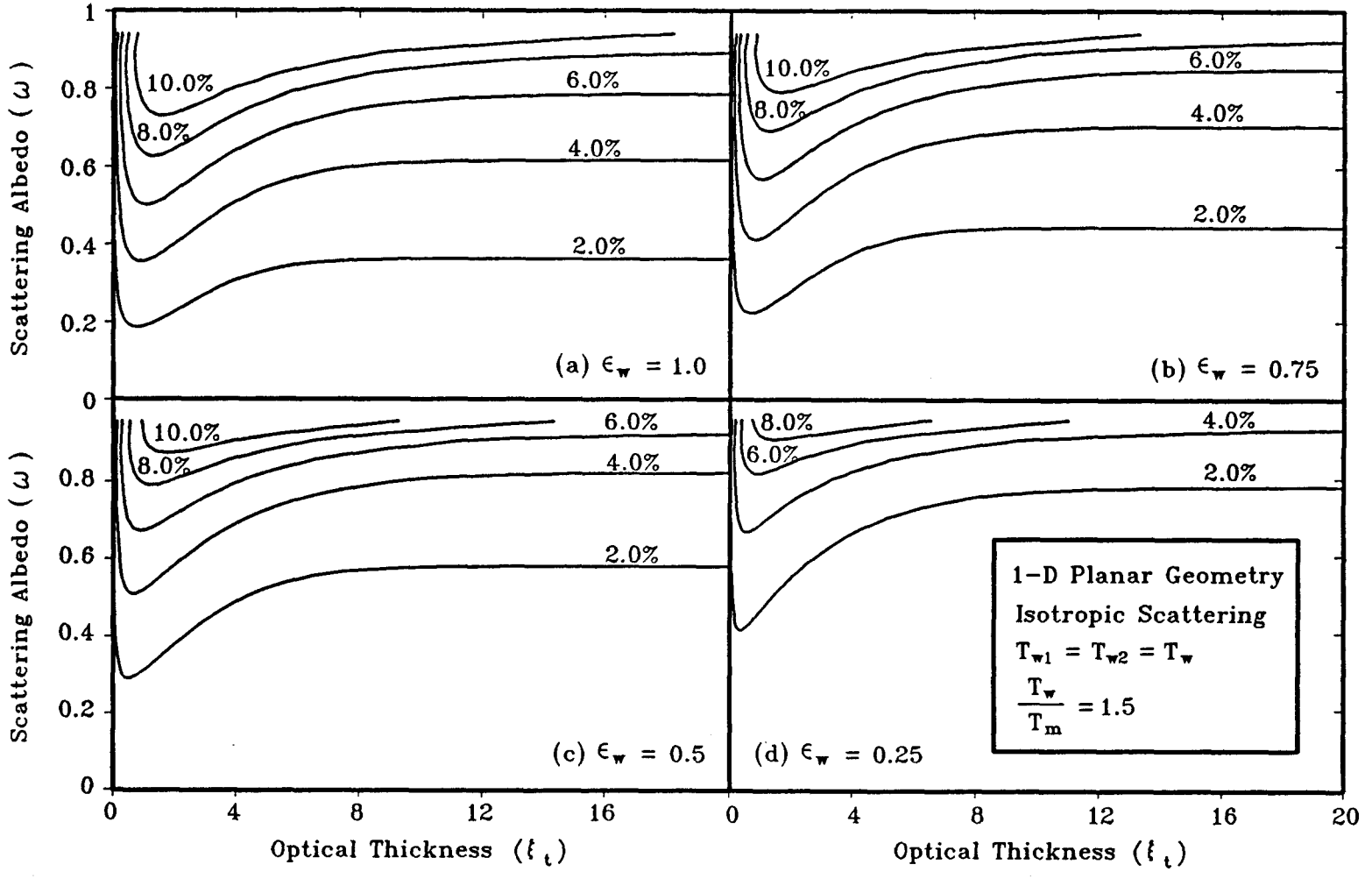

Fig. 2. Contours of constant percentage error in the net efflux, Eq. (22), predicted by the P_1 mapping technique for Case I of Table 1 and isotropic scattering.

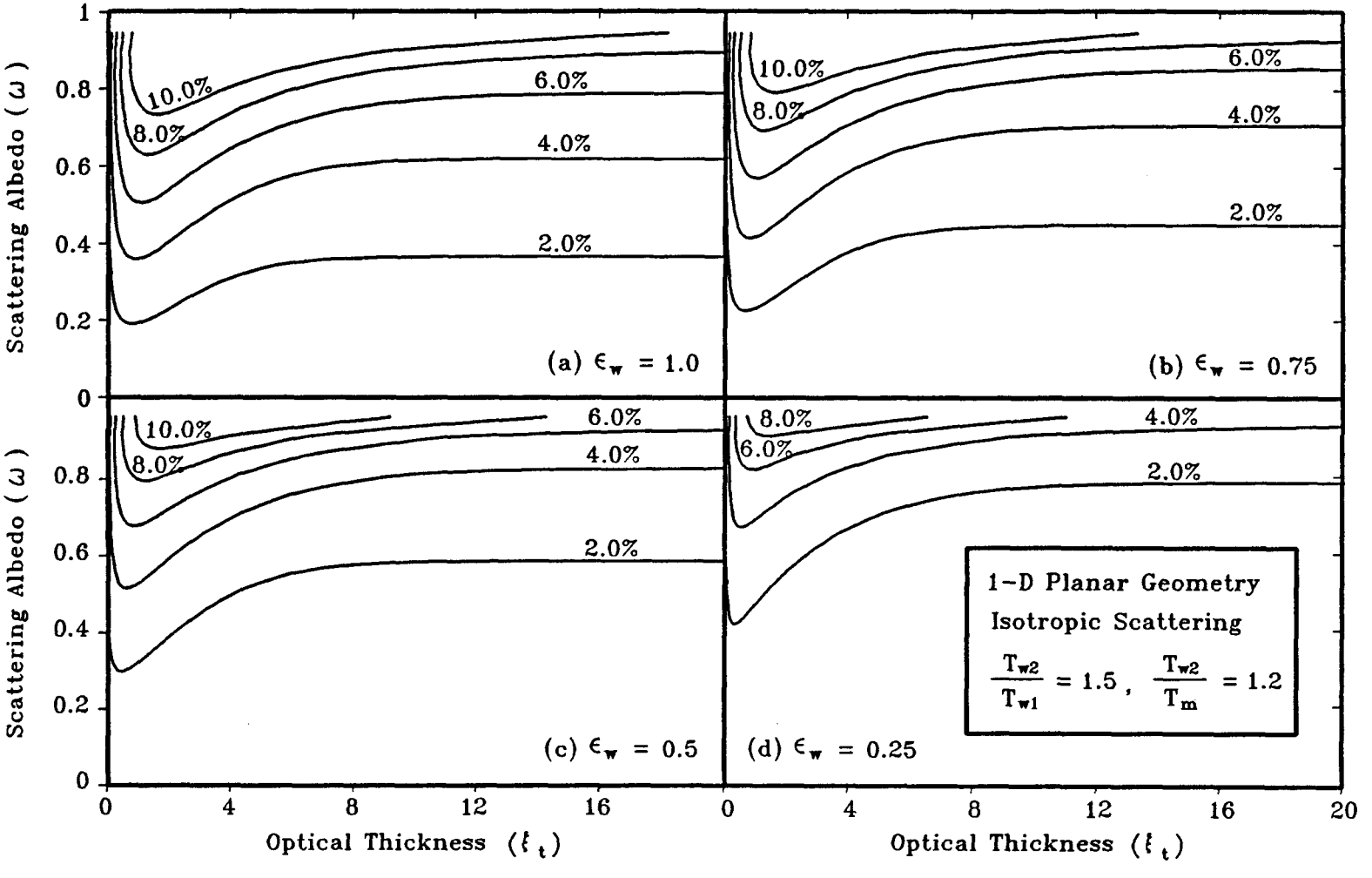

Fig. 3. Contours of constant percentage error in the net efflux, Eq. (22), predicted by the P_1 mapping technique for Case II of Table 1 and isotropic scattering.

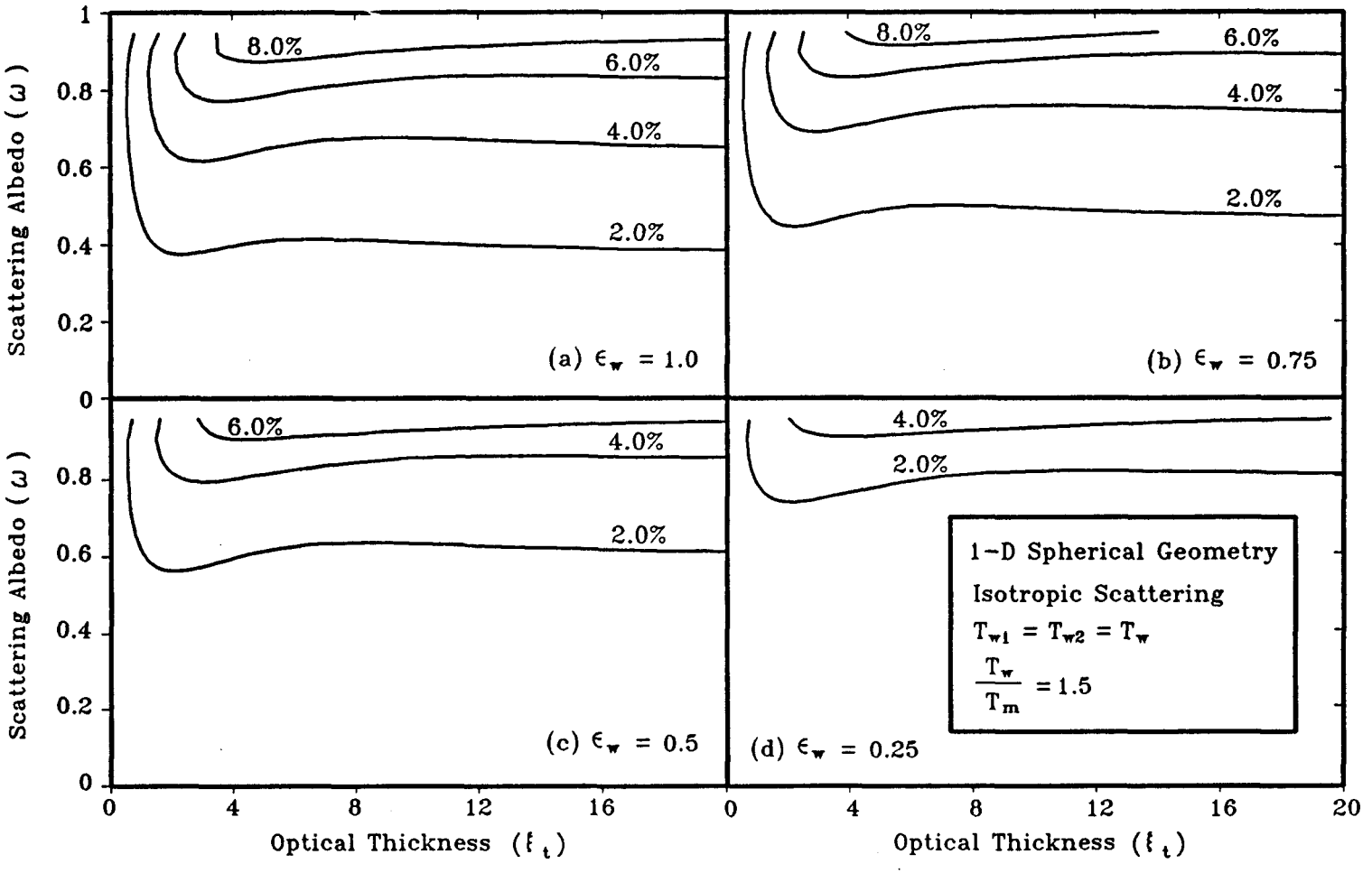

Fig. 4. Contours of constant percentage error in the net efflux, Eq. (22), predicted by the P_1 mapping technique for Case III of Table 1 and isotropic scattering.

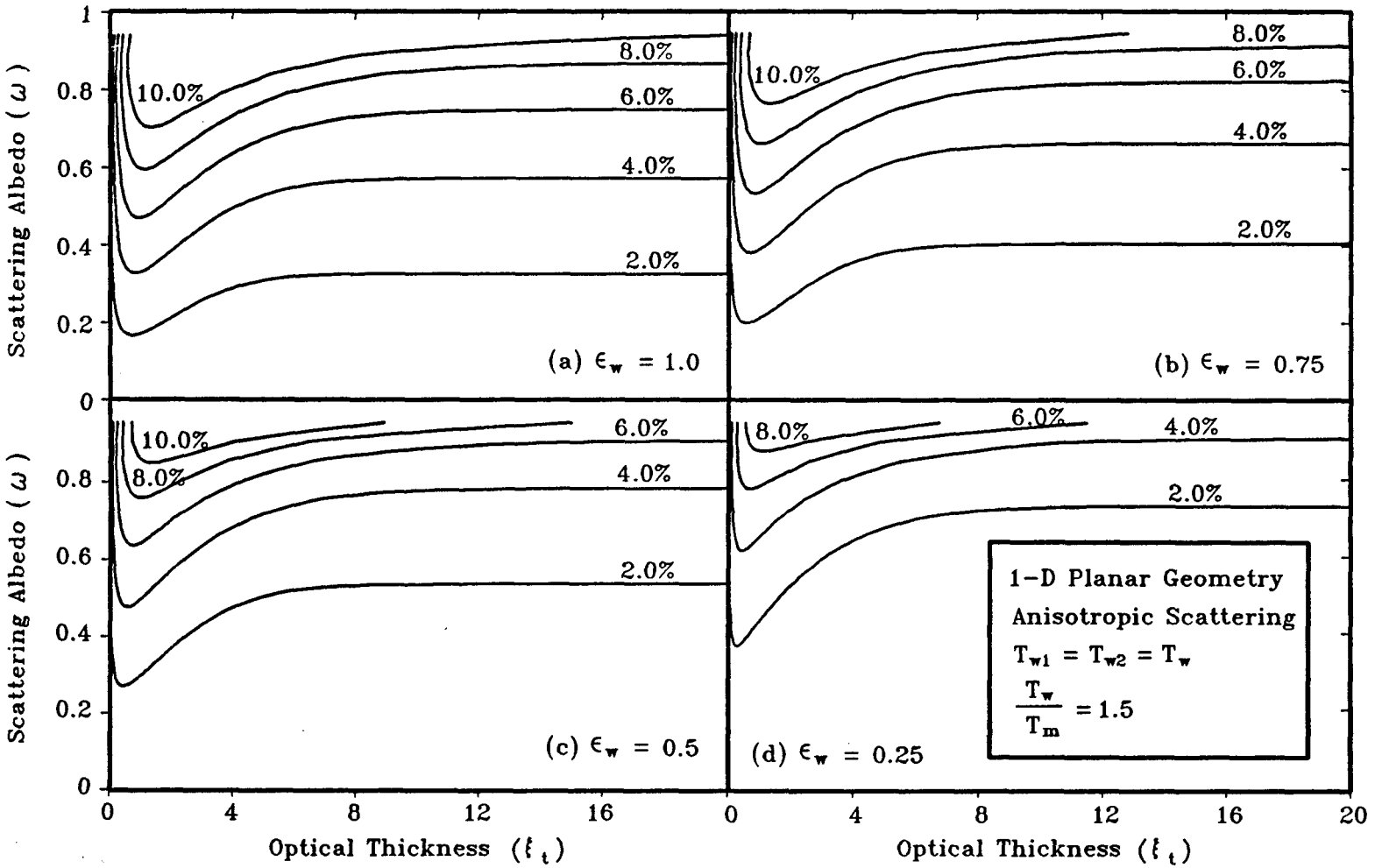

Fig. 5. Contours of constant percentage error in the net efflux, Eq. (22), predicted by the P_1 mapping technique for case I of Table 1 and anisotropic scattering.

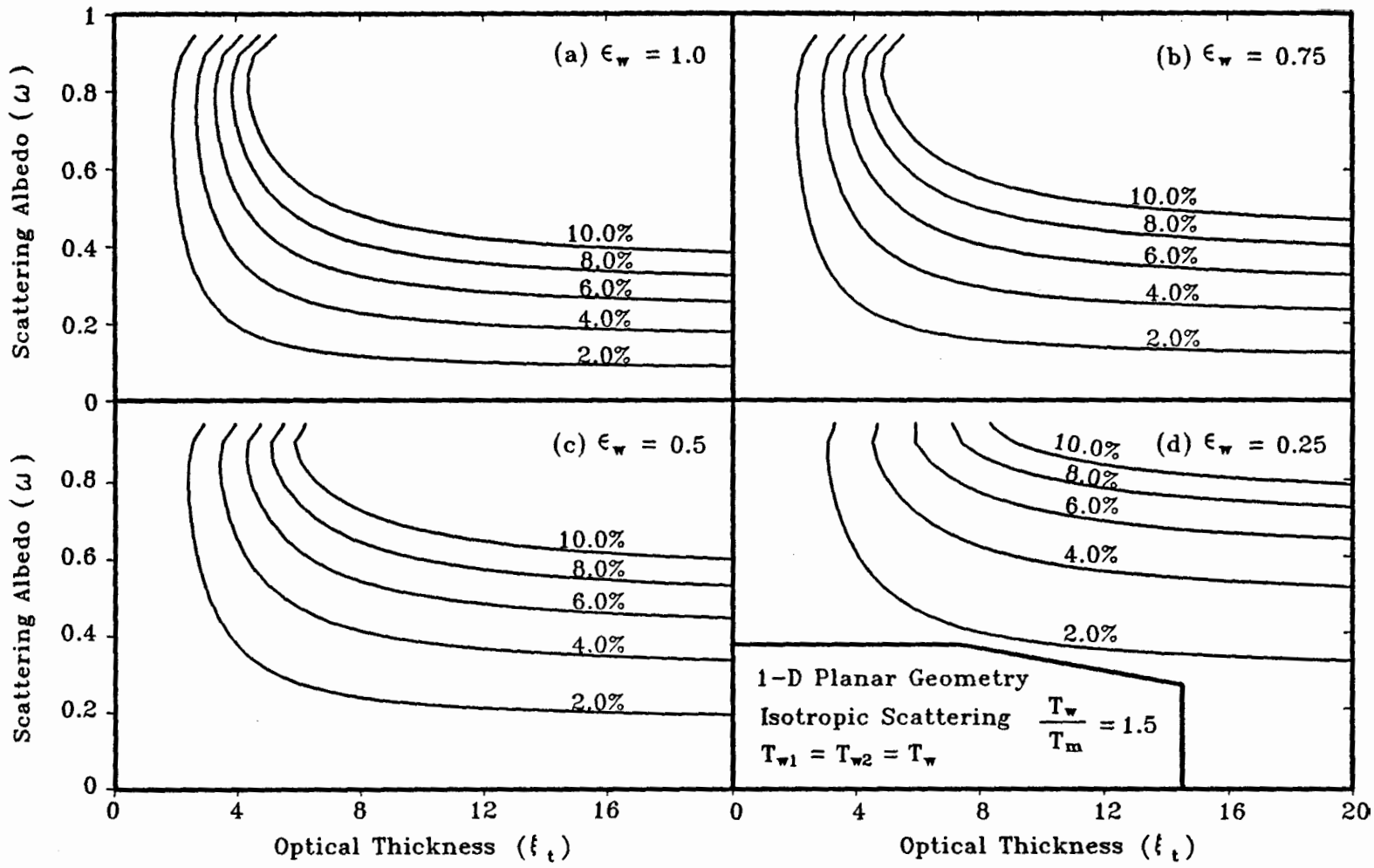

Fig. 6. Contours of constant percentage error in the net efflux, Eq. (22), predicted by the effective temperature technique for Case I of Table 1.

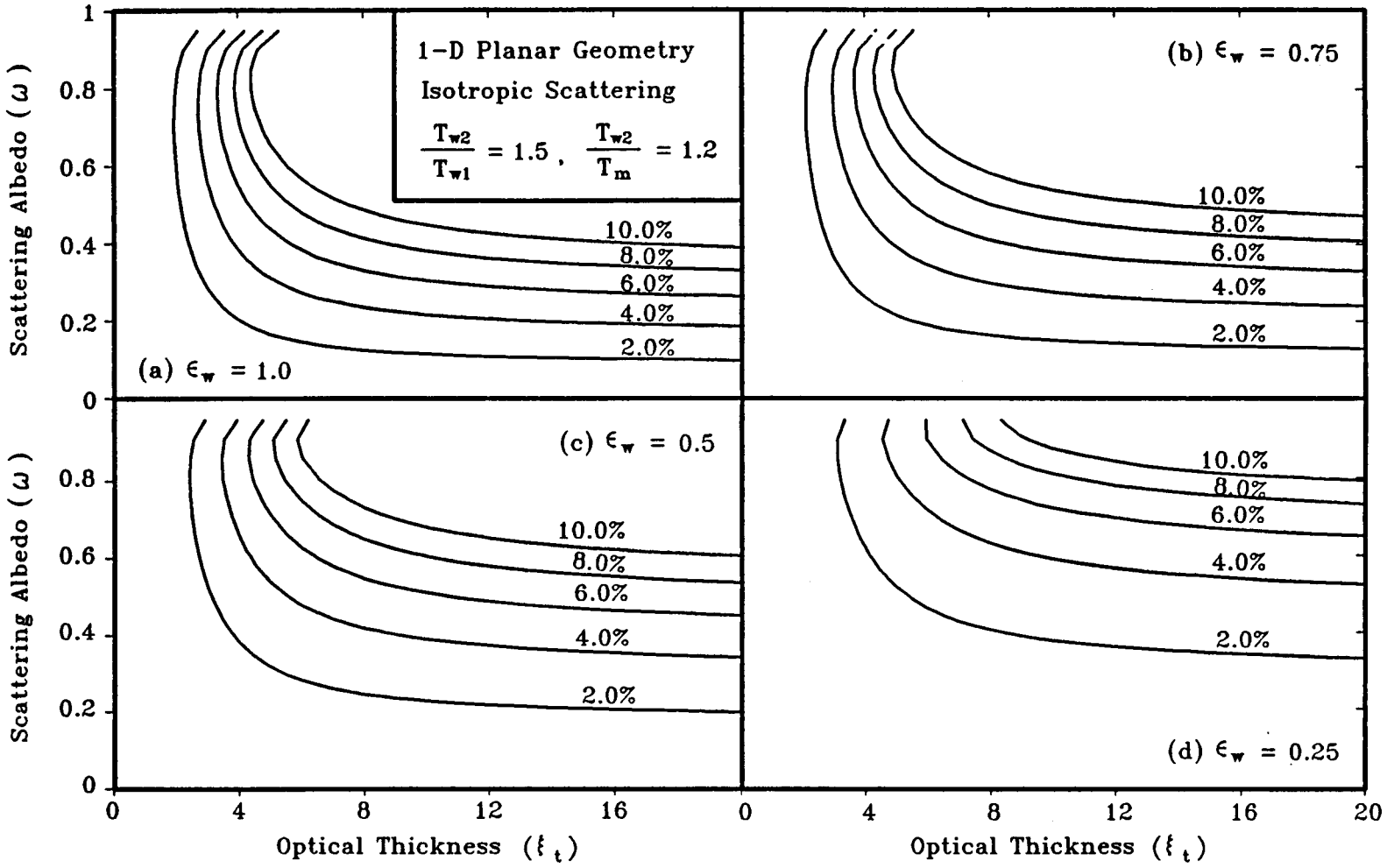

Fig. 7. Contours of constant percentage error in the net efflux, Eq. (22), predicted by the effective temperature technique for Case II of Table 1.

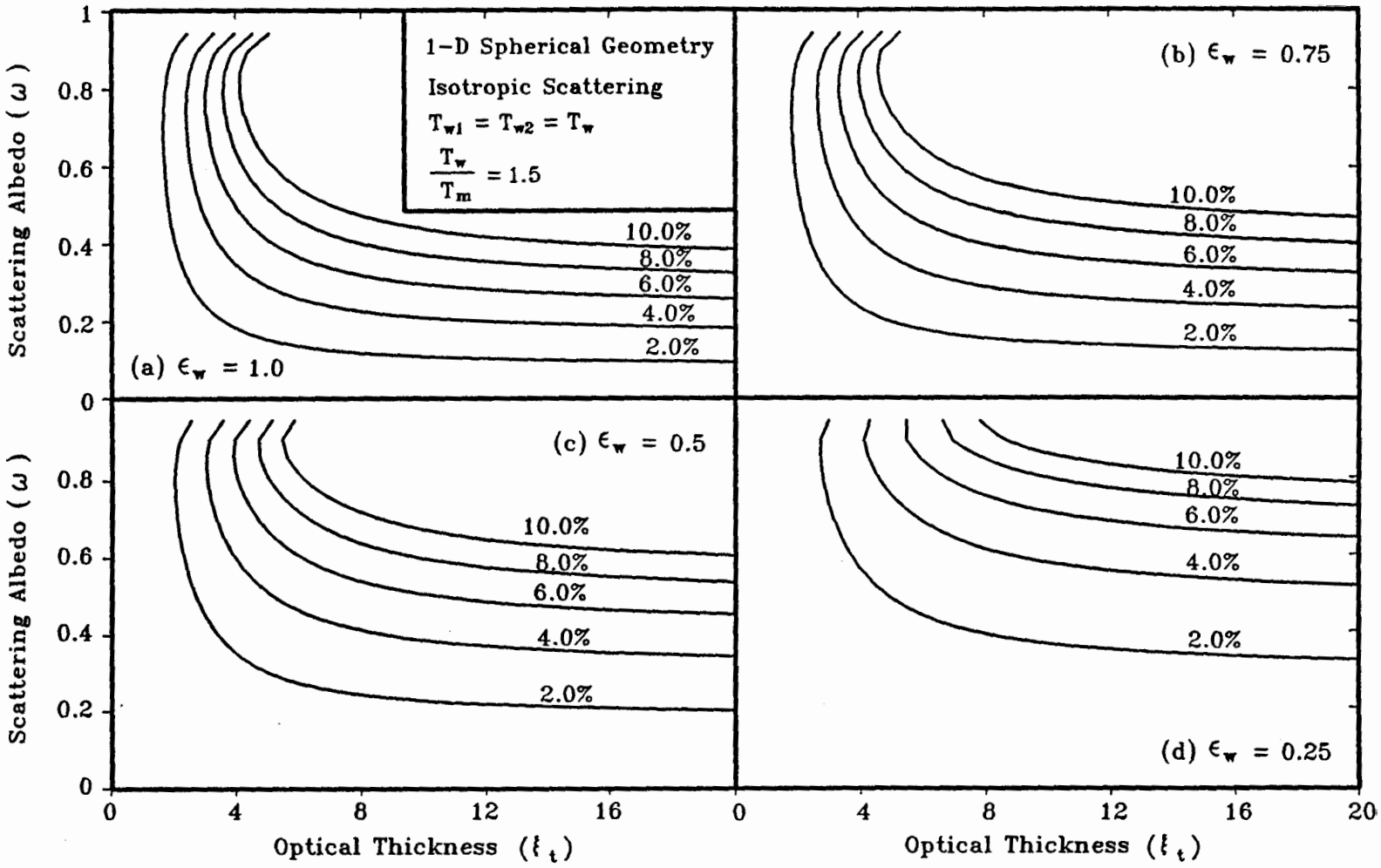

Fig. 8. Contours of constant percentage error in the net efflux, Eq. (22), predicted by the effective temperature technique for Case III of Table 1.